Isolation and Pharmacological Characterization of Six Opioidergic *Picralima nitida* Alkaloids

Simone M. Creed[*], Anna M. Gutridge[*], Malaika D. Argade, Madeline R. Hennessy, J. Brent Friesen, Guido F. Pauli, Richard M. van Rijn, and Andrew P. Riley

[*]Contributed equally

ABSTRACT

The seeds of the akuamma tree (*Picralima nitida*) have been used as a traditional treatment for pain and fever. Previous studies have attributed these effects to a series of indole alkaloids found within the seed extracts; however, these pharmacological studies were significantly limited in scope. Herein, an isolation protocol employing pH-zone-refining countercurrent chromatography is developed to provide six of the akuamma alkaloids in high purity and quantities sufficient for more extensive biological evaluation. Five of these alkaloids, akuammine, pseudo-akuammigine, picraline, akuammicine, and akuammiline, were evaluated against a panel of >40 central nervous system receptors to identify that their primary targets are the opioid receptors. Detailed *in vitro* investigations revealed one alkaloid as a potent kappa opioid receptor agonist and three alkaloids with micromolar activity at the mu opioid receptor. The mu opioid receptor agonists were further evaluated for analgesic properties but demonstrated limited efficacy in assays of thermal nociception. These findings contradict previous reports of the antinociceptive properties of the akuamma alkaloids and the traditional use of akuamma seeds as analgesics. Nevertheless, their opioid preferring activity does suggest the akuamma alkaloids provide distinct scaffolds from which to develop novel opioids with unique pharmacologically properties and therapeutic utility.

For centuries, morphine and its semi-synthetic derivatives have served as the cornerstone of pain management.[1] Opioid analgesics produce their powerful pain-killing effects through the activation of mu opioid receptors (μOR), one of three opioid receptors subtypes found throughout the central and peripheral nervous system.[2-3] Despite the effectiveness of opioid analgesics in acute and subacute settings, chronic pain remains an escalating and poorly managed health concern, affecting approximately 20% of adults worldwide.[4-5] Over the past two decades, opioid prescriptions for the treatment of chronic pain have risen dramatically despite their reduced effectiveness against chronic pain states.[3, 6] Unfortunately, the prolonged use of opioid analgesics elicits numerous adverse effects including respiratory depression, tolerance, and dependence.[1-3] Increased prescription and duration of use of short and long-acting/extended release opioids, combined with the side effect profile of opioid medications, has led to the current opioid epidemic characterized by >40,000 opioid overdose deaths per year since 2016.[7] To counter this trend, in 2016 the Center for Disease Control and Prevention provided new guidelines for the use of opioids in patients suffering from chronic pain with a focus on reducing and replacing opioids when possible.[8] This abrupt change has been effective in decreasing opioid prescriptions, but may have come at the expense of patients that were benefitting from their current opioid therapy and are now left undertreated.[9-10] It is within this setting that patients search for non-prescription alternatives such as *Mitragyna speciosa* (kratom) and *Picralima nitida* (akuamma) to self-medicate their pain and opioid withdrawal symptoms.[11-12]

Historically, natural products have served as an excellent source of novel scaffolds to initiate drug discovery efforts.[13] This is particularly true in the arena of pain and other disorders of the nervous system. Beyond the aforementioned analgesics derived from morphine, naturally occurring salicylic acid, capsaicin, and tetrahydrocannabinol have all been exploited for their pain killing effects.[14-15] For centuries, the akuamma tree has been used by natives of Western Africa to treat a variety of ailments including malaria, dysmenorrhea, and gastrointestinal disorders.[16] The seeds in particular have been used for their analgesic and antipyretic properties.[16] Notably, anecdotal reports indicate that, unlike traditional opioid analgesics, akuamma does not elicit euphoria, tolerance, or dependence. The analgesic effects of *P. nitida* seeds have been generally attributed to a class of indole alkaloids known as the akuamma alkaloids composed of akuammine (**1**), akuammidine (**2**), pseudo-akuammigine (**3**), akuammicine (**4**), akuammiline **(5)**, and picraline (**6**) (**Figure 1**).[17] In standard

nociception assays, both the ethanolic extract of *P. nitida* and isolated **3** demonstrated antinociceptive properties. While their potency is lower than morphine, the effects of **3** in these assays appeared to be longer lasting.[18-19]

Previous investigations indicated the antinociceptive effects of the akuamma alkaloids are produced through their interaction with the opioid receptors.[16-17] However, the scope of these studies was limited to the opioid receptors, excluded other nervous system receptors, and the rigor of those findings is linked to the suboptimal tools available at the time to study the pharmacology of the akuamma alkaloids. Moreover, several alkaloids found in relatively high abundance in *P. nitida* have remained uninvestigated. Nevertheless, the structural differences between the akuamma alkaloids and traditional opioid analgesics, paired with the reported mild side effect profile, suggests these alkaloids may exhibit unique signaling properties at the opioid receptors, and, therefore, may be promising starting points for the development of new pain management drugs. Thus, to provide additional insight into the effects of akuamma, we initiated studies focused on identifying an effective preparative purification strategy that permits the resolution of the six main alkaloids found within akuamma seeds in order to provide a more thorough investigation of their pharmacological activity *in vitro* and *in vivo*.

RESULTS AND DISCUSSION

Extraction and Isolation of Akuamma Alkaloids. To initiate our studies of the akuamma alkaloids, we sought to identify an isolation process capable of providing six alkaloids in high purity and quantities sufficient for *in vitro* and *in vivo* studies. Our initial efforts revealed **1** and **2** could be easily isolated in >95% purity through liquid-liquid extraction and selective crystallization. However, isolation of the other major alkaloids in this manner proved difficult due to their similar solubilities in organic solvents and their general tendency to form critical pairs, particularly at the preparative scale. Previous studies have employed combinations of normal-phase column chromatography, preparative TLC, high performance liquid chromatography (HPLC) and recrystallization to purify alkaloids present in *P. nitida* extracts.[17, 20-22] In our hands, normal phase chromatography resulted in poor separations of the alkaloids due to their remarkably similar polarities. Furthermore, irreversible adsorption of the alkaloids to the stationary phase severely decreased yields and was particularly problematic for compounds present in minor quantities.[23] Although semi-preparative reverse phase HPLC proved to be more effective in terms of compound resolution, severe limitation remained in overall efficiency in terms of time and resources for generating the quantities required for our studies.

The shortcomings of standard chromatography techniques led us to investigate countercurrent separation (CCS) to purify the *P. nitida* alkaloids. By eliminating the use of a solid stationary phase in favor of a continuous flow liquid-liquid partitioning system, both major forms of CCS, high speed countercurrent chromatography (HSCCC) and centrifugal partition chromatography (CPC), avoid the irreversible adsorption of compounds observed in solid phase-based liquid chromatography and allow for quantitative sample recovery.[24-26] Specifically, pH-zone-refining countercurrent chromatography (pHZR-CCC), which incorporates acid-base interaction of the two immiscible phases, is perfectly matched for the separation of basic alkaloids.[24-30] The method provides the benefit of a high loading capacity and produces highly concentrated fractions with minimal compound overlap.[24-26] Okunji *et. al.* have applied pHZR-CCC to the fruit rind of *P. nitida*, thus it stood to reason that their method could be adapted to isolate alkaloids found in the ground seeds.[23]

As with any liquid chromatography method, the selection of a suitable solvent system is critical to the outcome of the isolation. Solvent systems for pHZR-CCC require two immiscible solvents and typically incorporate the addition of co-solvents to modulate the partition coefficients of the compounds of interest. To select an applicable solvent system, we employed a straightforward partitioning method originally developed by Ito.[24] Five solvent systems comprised of 2-4 solvents, were modified with the addition of either acid (10 mM HCl) or base (10 mM TEA) and the partition coefficients of **3**-**6** was determined via HPLC to give K_{acid} and K_{base}, respectively (**Table 1**). Suitable *K* values for basic compounds such as the akuamma alkaloids should fit within the parameters $K_{acid} << 1$ and $K_{base} >> 1$.

Generally, pHZR-CCC has relied heavily on hexane-ethyl acetate-methanol water (HEMWat) and methyl *tert*-butyl ether (MTBE)-acetonitrile-water solvent systems. In particular, these solvent systems have been successfully employed in the separation of several classes of structurally similar indole alkaloids.[23, 27-30] Our initial investigations revealed that the less polar HEMWat systems were incompatible with the akuamma alkaloids due to the strong retention of compounds in the acidic aqueous phase and unexceptional base partition values for akuammiline and picraline. Turning to the 2:2:3 MTBE/ACN/H_2O system previously employed by Okunji, we observed $K_{acid}>1$ for **3** and **6**.[23] Further alterations to the solvent composition and rations revealed 1:1 EtOAc/H_2O and 3:1.5:4 MTBE/ACN/H_2O systems both proved to be viable solvent systems providing $K_{acid} << 1$ and $K_{base} >> 1$ for all four alkaloids. Of these two, the 1:1 EtOAc/H_2O system was selected as the most appropriate solvent

for pHZR-CCC based on the lower acid partition coefficient values and more consistent base partition coefficient values displayed, in addition to exhibiting a larger difference between the K_{acid} and K_{base} of the four alkaloids.

Having identified a promising solvent system, separation of the dichloromethane fraction with pHZR-CCC was first attempted in descending mode using an acidic aqueous mobile phase. Using this method, **4** was first to elute, followed by **3** and subsequently mixed fractions of **5** and **6**. As expected, performing the run in ascending mode with the basic organic layer as the mobile phase, the order of elution was observed to be the exact opposite of the descending method. Reversing the elution mode facilitated easier concentration of the fractions collected and allowed the alkaloids of interest to elute much earlier in the run.

A plot of the pH values for each fraction produced a series of alternating zones of increasing pH and plateaus which is characteristic of the pHZR-CCC. When overlaid onto the UV-Vis chromatograms, the elution of major alkaloids was observed to coincide with a plateau on the pH curve, presumably at the points where the pH is roughly equal to their isoelectric point (**Figure 2).** While initially fractions were collected in 15 mL volumes, reduction of the volume to 7.5 mL led to significant increases in alkaloid purity. From a 1.2 g sample of the dichloromethane fraction, this process directly provided 130 mg of pseudo-akuammigine and 145 mg of akuammicine in high purity. Despite significant attempts to optimize the solvent system and pHZR-CCC conditions, picraline and akuammiline consistently co-eluted as ~1:1 mixture. Fortunately, this mixture could be easily separated on silica gel via flash chromatography to provide 61 mg of **5** and 90 mg of **6**. Notably, attempts to directly purify the dichloromethane fraction via flash chromatography were unsuccessful due to considerable co-elution of multiple alkaloids, thus highlighting the necessity to first simplify the fraction via pHZR-CCC.

Once isolated, the purified alkaloids were identified as **1**, **2**, **3**, **4**, **5**, and **6**by comparison of the ^{1}H and ^{13}C NMR spectra to literature values.[31-33] In particular, the comparison of the ^{13}C NMR chemical shifts to literature values revealed an average absolute difference of 0.24 ppm, with major differences arising from subtle solvent-dependent changes in chemical shifts (**Supplementary Tables 1-6**). In addition to this agreement with literature values, the spectral data are consistent with previously reported structures.

Identification of Major Drug Targets Through the Psychoactive Drug Screening Program (PDSP). With the akuamma alkaloids in hand, five of the isolated alkaloids were evaluated via the Psychoactive Drug Screening Program (PDSP) to determine possible receptor targets for their purported biological effects. **1** and **3-**

6 were first assessed at a single concentration (10 μM) for their ability to displace radiolabeled ligands from a diverse panel of human G-protein coupled receptors, ion channels, and transporters. In this primary screen, all five akuamma alkaloids inhibited [^{3}H]-SCH-23390 from the dopaminergic D_5 receptor and [^{3}H]-U69,593 from the κOR (**Figure 3**). **1**, **3**, and **4** also displaced [^{3}H]-DAMGO from the μOR, whereas **5** and **6** produced significantly less displacement in these assays. All five of the tested alkaloids produced minimal inhibition of [^{3}H]-DADLE binding at the δOR. Although additional displacement was noted for several of the serotonergic and the histaminergic H_3 receptors these were generally low levels of inhibition (<60%). In contrast to **1**, **3**, **5**, and **6**, which appear to be moderately selective for the opioid and D_5 receptors, the primary binding data indicate **4** is considerably more promiscuous.

To validate these potential receptor targets, secondary binding experiments were carried out by the PDSP to determine binding affinities (K_i) for each receptor-ligand pair demonstrating >50% inhibition in the primary screen. Notably, the D_5 K_i >10 μM for all five alkaloids, indicating a false positive in the primary screen data (**Supplementary Table 7**). Conversely, **1** and **3** possess considerable affinity at the μOR (K_i = 0.76 μM and 1.0 μM, respectively) while **4** and **5** bind with sub-micromolar affinity to the κOR (K_i = 0.17 μM and 0.40 μM, respectively). These data generated from the cloned human opioid receptors are in good agreement with those reported by Menzies *et. al.* using guinea pig brain homogenates.[17] Furthermore, the data strongly support the hypothesis that any observed biological effects of akuamma likely occur through interactions with the opioid receptors.

Characterization of *in vitro* Pharmacology of Akuamma Alkaloids. Having established that the alkaloids target opioids receptors, we next assessed the affinity and potency of akuamma alkaloids for binding, activation of G-protein and β-arrestin 2 recruitment at the μOR, κOR, and δOR in our own cellular assays. In general, the alkaloids had higher affinity and activity at the μOR and κOR, relative to δOR (**Figure 4A-I**), confirming the results from the PDSP. For all cellular characterization assays, the alkaloids had weaker affinity, potency and efficacy when compared to reference ligands DAMGO, U50,488, and leu-enkephalin (**Figure 4A-I**). More specifically, at the μOR, **1-3** had the highest binding affinities with K_is of 0.30, 0.32 and 0.59 μM, respectively (**Figure 4A, Table 2**). The binding affinity for these compounds was reflected in their increased potency and efficacy in the cAMP inhibition assay at the μOR, relative to the other alkaloids, with **1** and **2** producing IC_{50}s of 2.6 and 3.14 μM (**Figure 4D, Table 2**). **4**, **5** and **6** all had minimal cAMP inhibition at μOR,

which is reflective of their relatively lower binding affinity at the receptor (**Figure 4A, 4D**). The alkaloids had non-determinable β-arrestin 2 recruitment at the μOR, but **2** did show minimal recruitment at the highest concentration tested (**Figure 4G**). At the κOR, **4** had the highest binding affinity with a K_i of 89 nM, which mirrors its potency in the cAMP assay with an IC_{50} of 240 nM (**Figure 4B, 3E, Table 2**). **1**, **3**, **5** and **6** all had similar binding affinity at the κOR, while **2** had the least affinity (**Figure 4B, Table 2**). Notably, **1** did not inhibit cAMP production, suggesting it possesses antagonistic or inverse agonistic properties at the κOR. Within the tested dose-range, the alkaloids minimally recruited β-arrestin at the κOR, but followed the general trend that β-arrestin 2 recruitment was most apparent in alkaloids that display the strongest binding affinity (**Figure 4H, Table 2**). Compared to the μOR and the κOR, binding affinity, as well as potency and efficacy of the compounds in the cAMP inhibition assay, was lower at the δOR (**Figure 4C,3F, Table 2**). Similar to the other receptors, there was non-determinable β-arrestin recruitment by the alkaloids at the δOR, although **2** did show minimal recruitment at the highest concentration tested (**Figure 4I**).

The comparable binding results reported in Menzies *et al.*, in the PDSP screen shown in **Figure 1**, and in the radioligand binding assays shown in **Figure 4A-C** confirm that the akuamma alkaloids are able to interact with opioid receptors.[17] The results from the *in vitro* signaling assays in **Figure 4D-I** further demonstrate that the alkaloids not only bind to opioid receptors but can elicit intracellular, inhibitory G-protein activity as well as β-arrestin 2 recruitment. The potency for the akuamma alkaloids in the β-arrestin 2 recruitment assay was too weak to calculate bias factors. Inspection of the functional responses at κOR suggests that the efficacy of β-arrestin 2 recruitment correlates with the potency for G-protein mediated cAMP inhibition; **4** is the most efficacious recruiter, while **2** is the weakest. Based on their inherent opioid activity, moving forward, more potent and selective opioids may be discovered using the akuamma alkaloids as a scaffold for drug design.

***In vivo* Characterization of Antinociceptive Effects of Akuamma Alkaloids.** Given the ability of the akuamma alkaloids to bind to and activate the μOR, we hypothesized that the reported analgesic efficacy of the akuamma plant may be primarily exerted by these μOR-activating akuamma alkaloids. As **3** has previously been demonstrated to be antinociceptive in Wistar rats when administered *per os* (p.o.; 5 mg/kg), we set out to reproduce these findings in mice (**Supplementary Table 8**).[19] In our observations, **3** did not produce antinociception in mice at 5 mg/kg dose (p.o.) in the tail flick and hot plate assays of thermal nociception at any of the timepoints tested (**Figure 5A-B**). In this experiment, subcutaneously (s.c.) administered morphine (6

mg/kg) served as a positive control and produced significant antinociception at the 30 min timepoint. However, when 5 mg/kg **3** was administered subcutaneously, minimal yet statistically significant antinociception was measured at 30 minutes in both nociception assays, as well as at 60 minutes in the tail-flick assay (**Figure 5C-D, Supplementary Table 9**). Notably, a 10 mg/kg dose of **3** (s.c.) also failed to produce antinociception at 30 minutes (**Figure 5C, D**).

Because **1** and **2** had slightly higher potencies than **3** at the μOR, they were also tested for antinociceptive properties. Alkaloid **1** was tested at 3, 10, 30, and 60 mg/kg doses (s.c.). In the tail flick assay, minimal yet statistically significant antinociception was measured at 110 minutes for the 3 mg/kg dose, and at 30 minutes for the 60 mg/kg dose (**Figure 6A, Supplementary Table 10**). In the hotplate assay, minimal yet statistically significant antinociception was measured at 110 minutes for the 3 mg/kg dose, at 60 minutes for the 30 mg/kg dose, and at 30 minutes for the 60 mg/kg dose (**Figure 6B, Supplementary Table 10**). Alkaloid **2** was tested at 3, 10, and 30 mg/kg doses (s.c.). In the tail flick assay, minimal yet statistically significant antinociception was measured at 50 minutes for the 10 mg/kg dose, and at 30 minutes for the 30 mg/kg dose (**Figure 6C, Supplementary Table 11**). In the hotplate assay, minimal, yet statistically significant, antinociception was measured at 110 minutes for the 3 mg/kg dose (**Figure 6D, Supplementary Table 11**). For both **1** and **2**, dose-dependent increases in antinociception were not observed reproducibly between nociception assays, and there was no general trend in the time-course of antinociceptive effect. To explore whether the route of administration for **1** and **2** would influence antinociceptive effect, oral dosing was also examined. However, no antinociception was measurable, indicating that metabolism of the compounds is unlikely to contribute to potential effects as has been previously proposed (data not shown).[19]

In a previous study in rats, the antinociceptive effects of **3** differed kinetically from those produced by morphine, with antinociceptive activity for **3** peaking at 180 minutes when administered p.o..[19] To account for potential delayed onset in antinociception for akuamma alkaloids we tested nociception in our mice 50 and 110 minutes following s.c. administration with **1** and **2**. However, with continued testing and after failing to detect convincing levels of antinociception, we adjusted testing of higher doses to 30 and 60-75 minutes in an attempt to capture either a rapid or delayed peak in antinociceptive efficacy. To ensure that the s.c. route of administration was not contributing to our lack of detecting any antinociception, we also measured nociception following p.o. administration of **1**-**3**, yet still did not observe convincing levels of antinociception as was demonstrated by

Duwiejua *et al*.[19] The lack of antinociception with p.o. administration leads us to believe that metabolism of the akuamma alkaloids does not greatly contribute to their purported antinociceptive effects. The incongruous antinociceptive findings between our study and previous research may be explained by species differences: in this study, C57BL/6 mice were used, whereas Wistar rats were used in the previous study.[19]

CONCLUSION

Natural products, and in particular plant alkaloids, are a well-known source for medicinal compounds with analgesic potency. Most familiar are the opioids found in *Papaver somniferum*, but more recently *Mitragyna speciosa* has gained recognition in Western society as an alternative source of naturally occurring analgesics. Here we provided a detailed investigation of the isolation of six abundant, yet chromatographically very similar, alkaloids from the seeds of *Picralima nitida*, a traditional plant with reported analgesic properties. Using high-purity isolates, this study undertook a detailed characterization of the pharmacology of the isolated akuamma alkaloids in mammalian cells, and performed an evaluation of their antinociceptive effects in mice.

Our cellular signaling characterization of the akuamma alkaloids at the opioid receptors agrees with previous findings but enhances the previous assessment with our reported analysis of intracellular signaling properties, particularly β-arrestin recruitment, at the opioid receptors as well as binding capability to non-opioid receptors.[17] We find that the akuamma alkaloids potency was too weak to accurately determine β-arrestin recruitment, however, several alkaloids display significant recruitment (>25%) at the highest dose that could be tested. The pharmacological profile of the akuamma alkaloids stands in contrast to the kratom alkaloids, particularly 7-hydroxymitragynine, which can be classified as a highly potent and G-protein-biased μOR agonist.[34] Of all the akuamma alkaloids investigated, **4** stands out as being relatively potent at the κOR. The promiscuity of **4** for other receptors is conceivably problematic; however, it has potential for serving as a scaffold for developing novel κOR agonists.

In our analysis of akuamma's antinociceptive properties, we report limited antinociceptive efficacy of three akuamma alkaloids: **1**-**3**. While the observed limited antinociceptive efficacy does not support akuamma's traditional use for pain relief, and is not congruous with a previous report of potent antinociception by **3** in rats,[19] this apparent contradiction is by far not unusual for investigations of ethnomedically used plants; as we and others have demonstrated, compound abundance and pharmacological relevance are not necessarily

correlated,[35-37] and even very minor components or even impurities can be responsible for the observed biological activity.[38] Thus, while these studies provide detailed insight into the pharmacology of six highly abundant alkaloids present in the *P. nitida* extracts, other components present in lower abundance may possess potent antinociceptive activity. Furthermore, it is possible that pharmacokinetic and/or pharmacodynamic differences between rats and mice may account for the discrepant antinociceptive responses for the akuamma alkaloids in Wistar rats and C57BL/6 mice. Future studies should explore the pharmacokinetics of the akuamma opioids and akuamma metabolites in mice, confirm the reported antinociceptive effect in rats, and investigate potential synergistic interaction of the akuamma alkaloids *in vivo*. Additionally, despite the limited antinociceptive efficacy reported here, the unique structural features of the akuamma alkaloids provides opportunities to study the opioid receptors. By exploring the structure-activity relationships of these scaffolds and developing synthetic analogs, particularly those with improved pharmacokinetic and pharmacodynamic properties, the akuamma alkaloids may be transformed into useful pharmacological probes of the opioid receptors and to gain utility in treating pain and other disorders.

EXPERIMENTAL SECTION

General Experimental Procedures. All solvents and reagents were purchased from commercial sources and used directly without further purification. Akuamma seed powder was purchased from Relax Remedy. ^{1}H and ^{13}C NMR spectra were recorded on Bruker 400 MHz spectrometer and referenced to the residual solvent peaks ($CHCl_3$: ^{1}H δ=7.26, ^{13}C δ=77.16 ppm; D_2HCOD: ^{1}H δ= 3.31, ^{13}C δ=49.00 ppm) High-resolution mass spectra were obtained on a Shimadzu LCMS-IT-TOF and observed values are within 5 ppm of calculated exact masses of the indicated ions. High-performance liquid chromatography was conducted on an Agilent 1260 Infinity II fitted with a DAD detector and a Phenomenex Luna Omega PS-C18 column (100 x 4.6 mm). A gradient of acetonitrile/water (20-45%) each containing 0.1% formic acid with a flow rate of 1 ml/min was used. The purity of all compounds was determined to be >95% as determined by HPLC.

Drugs. Leu-enkephalin, forskolin, and morphine sulfate pentahydrate were purchased from Sigma Aldrich (St. Louis, MO, USA). (2S)-2-[[2-[[(2R)-2-[[(2S)-2-Amino-3-(4-hydroxyphenyl)propanoyl]amino] propanoyl] amino]acetyl]-methylamino]-N-(2-hydroxyethyl)-3-phenylpropanamide (DAMGO), and 2-(3,4-dichlorophenyl)-N-methyl-N-[(1R,2R)-2-pyrrolidin-1-ylcyclohexyl]acetamide (U50,488) were purchased from Tocris Bioscience (Bio-techne Corporation, Minneapolis, MN, USA). [^{3}H]DAMGO (49.2 Ci/mmole, lot#2573313),

[^{3}H]U69,593 (60 Ci/mmole, lot#2367921), and [^{3}H]DPDPE (53.7 Ci/mmole, lot#2376538) were purchased from Perkin Elmer (Waltham, MA, USA).

Preparation of Dichloromethane Fraction, Pure Akuammine (1), and Akuammidine (2). Akuamma seed powder (250 g) was allowed to stir for two hours in methanolic hydrochloride solution (400 mL). Subsequently, the seed powder was filtered, and the filtrate was evaporated to dryness under reduced pressure. The resulting extract was dissolved in aqueous hydrochloric acid (400 mL, 2N), washed with hexanes (3x400 mL), and extracted with dichloromethane (3x400 mL). The combined dichloromethane layers were evaporated to dryness under vacuum to provide the crude dichloromethane fraction (3.356 g). The aqueous layer was brought to pH=12 with 28% ammonium hydroxide, washed with hexanes (1x400 mL), and extracted with ethyl ether (3x400 mL). The combined ethereal layers were dried over magnesium sulfate and concentrated under vacuum to provide a mixture of akuammine and akuammidine. This mixture was washed with cold acetone to precipitate **1** as a white solid (472 mg). The acetone filtrate was concentrated under vacuum and the resulting residue recrystallized in dichloromethane to yield crystalline **2** (15.0 mg).

Akuammine (1): white solid, ^{1}H NMR ($CDCl_3$, 400 MHz) δ 6.69 (1H, d, *J* = 2.44 Hz), 6.61 (1H, dd, *J* = 8.3, 2.5 Hz), 6.50 (1H, d, *J* = 8.3 Hz), 5.43 (1H, q, *J* = 6.9 Hz), 4.15 (1H, s), 3.94 (2H, m), 3.82 (3H, s), 3.66 (2H, m), 3.50 (1H, s), 3.32 (1H, ddd, *J* = 14.5, 14.5, 5.8 Hz), 2.86 (1H, d, *J* = 16.8 Hz), 2.79 (3H, s), 2.59 (1H, dd, *J* = 13.5, 5.7 Hz), 2.34 (1H, d, *J* = 13.7 Hz), 2.07 (1H, ddd, *J* = 13.9, 3.4, 1.8 Hz), 1.54 (3H, dd, *J* = 7.0, 2.0), 1.50 (1H, dd, *J* = 15.3, 4.1 Hz); ^{13}C NMR ($CDCl_3$, 100 MHz) δ 172.0, 149.9, 145.4, 141.9, 140.4, 118.4, 113.4, 111.3, 110.2, 104.1, 74.0, 58.3, 54.4, 53.7, 52.5, 52.0, 50.4, 40.9, 31.0, 29.4, 27.9, 12.9.

Akuammidine (2): ^{1}H NMR (CD_3OD, 400 MHz) δ 7.39 (1H, d, *J* = 7.7 Hz), 7.29 (1H, d, *J* = 8.0 Hz), 7.06 (1H, t, *J* = 7.4 Hz), 6.98 (1H, t, *J* = 7.4 Hz), 5.47 (1H, q, *J* = 6.7 Hz), 4.25 (1H, d, *J* = 9.7 Hz), 3.80 (1H, d, *J* = 9.7 Hz), 3.68-3.63 (2H, m), 3.54 (1H, d, *J* = 16.8 Hz), 3.44 (1H, dd, *J* = 16.8, 3.3 Hz), 3.27 (1H, d, *J* = 3.2 Hz), 2.96 (3H, s), 2.88-2.84 (2H, m), 2.72 (1H, ddd, *J* = 13.1, 4.2, 1.6 Hz), 1.92 (1H, t, *J* = 11.6 Hz), 1.71 (3H, d, *J* = 6.8 Hz); ^{13}C NMR (CD_3OD, 100 MHz) δ 173.3, 137.1, 137.1, 136.4, 126.5, 120.7, 118.3, 117.2, 116.9, 110.6, 104.7, 67.6, 57.6, 54.7, 51.3, 50.6, 50.2, 28.9, 28.7, 23.6, 11.9.

pH-Zone Refining Countercurrent Chromatography of the Dichloromethane Fraction. The pH-Zone Refining Countercurrent Chromatography was performed on a SCPC-250 (Gilson Incorporated, Middleton, WI USA) chromatograph equipped with a 266 mL rotor. The rotation speed could be adjusted from 500 to 3000 rpm.

Samples were injected through a 20 mL sample loop. The detection was performed by a UV-Vis DAD detector. Fractions were collected with a Gilson-Armen Fraction Collector LS-5600. Chromatographic data were acquired by using the Gilson-Armen Glider CPC Control Software V2.9.2.9 and then transferred to an Excel worksheet for further processing.

The optimal solvent system was determined by evaluation of the acid and base partition coefficients of the alkaloids of interest using guidelines described by Ito.[18] Five different solvent system formulations were tested, with triethylamine (TEA) and hydrochloric acid (HCl) added to the upper (organic) and lower (aqueous) phases, respectively. Partition coefficients were determined by comparing the area under the curve for the HPLC peaks produced by akuammicine, akuammiline, pseudo-akuammigine, and picraline (**Table 1**).

The pH-zone-refining countercurrent chromatography separation was prepared by thoroughly mixing equal volumes of ethyl acetate and water in a 2 L separatory funnel and allowing the layers to separate. The ethyl acetate layer was basified with TEA to a final concentration of 10 mM to be used as the upper phase. The aqueous lower phase was adjusted to a final concentration of 8 mM with hydrochloric acid. The dichloromethane extract (1.2 g) was dissolved in 10 mL of upper phase with less than 1 mL of the lower phase to aid solubility and loaded into a 20 mL sample loop. An additional 5 mL of upper phase was used to rinse the sample vial and added to the sample loop. The instrument column was filled with the lower phase at a rotation speed of 500 rpm. The rotation speed was increased to 3000 rpm and the sample was introduced into the column. The basic ethyl acetate was pumped through the coil at a flow rate of 10 mL/min with elution in ascending mode. Elution was monitored at 254 nm, 284 nm and 330 nm. Fractions were collected in 7.5 mL quantities. After elution, the pH of each fraction was measured using a benchtop pH meter (Mettler Toledo) and fraction contents were evaluated using TLC. All fractions were dried with sodium sulfate, concentrated under vacuum, and analyzed by ^{1}H NMR. Fractions containing pure, individual alkaloids were combined separately to provide **3** (130 mg) and **4** (145 mg). Fractions containing a mixture of picraline and akuammiline were combined and further purified by flash column chromatography eluting with 0-2% MeOH/$CHCl_3$ containing 1% TEA to yield pure samples of **5** (61 mg) and **6** (90 mg).

Pseudo-akuammigine (3): ^{1}H NMR ($CDCl_3$, 400 MHz) δ 7.14 (1H, td, *J* = 11.5, 1.2 Hz), 7.09 (1H, d, *J* = 7.4 Hz), 6.75 (1H, td, *J* = 11.2, 0.8 Hz), 6.66 (1H, d, *J* = 7.8 Hz), 5.44 (1H, q, *J* = 7.0 Hz), 4.23 (1H, br s), 4.01-3.93 (2H, m), 3.84 (3H, s), 3.67-3.58 (2H, m), 3.51 (1H, br s), 3.34 (1H, ddd, *J* = 14.5, 14.5, 5.8 Hz), 2.91 (1H,

d, *J* = 12.5 Hz), 2.85 (3H, s), 2.61 (1H, dd, *J* = 13.4, 5.7 Hz), 2.35 (1H, d, *J* = 13.4 Hz), 2.12-2.06 (1H, m), 1.55 (3H, dd, *J* = 7.0, 2.2 Hz), 1.50 (1H, dd, *J* = 15.1, 4.2 Hz); ^{13}C NMR ($CDCl_3$, 100 MHz) δ 172.2, 151.8, 142.3, 139.3, 127.4, 122.4, 119.9, 118.2, 109.8, 103.9, 74.4, 58.4, 54.6, 53.7, 52.7, 51.9, 50.8, 41.0, 31.3, 29.0, 28.0, 12.9.

Akuammicine (4): off-white solid, ^{1}H NMR ($CDCl_3$, 400 MHz) δ 9.01 (1H, br s), 7.25 (1H, d, *J* =7.3 Hz), 7.16 (1H, t, *J* = 7.7 Hz), 6.91 (1H, t, *J* = 7.5 Hz), 6.83 (1H, d, *J* = 7.8 Hz), 5.37 (1H, q, *J* = 6.8 Hz), 4.06 (1H,s), 3.95 (1H, s), 3.91 (1H, d, *J* = 15.2 Hz), 3.82 (3H, s), 3.28 (1H, td, *J* = 18.8, 5.6 Hz), 3.03 (1H, dd, *J* = 12.3, 6.7 Hz), 2.97 (1H, d, *J* = 15.1 Hz), 2.51 (1H, ddd, *J* = 12.6, 12.6, 6.8 Hz), 2.43 (1H, ddd, *J* = 13.4, 3.7, 2.2 Hz), 1.84 (1H, dd, *J* = 12.6, 5.7 Hz), 1.63 (3H, d, *J* = 6.9 Hz), 1.32 (1H, ddd, *J* = 13.5, 2.8, 2.8); ^{13}C NMR ($CDCl_3$, 100 MHz) δ 167.9, 167.5, 143.4, 138.4, 136.7, 127.9, 121.5, 121.1, 120.9, 109.5, 101.3, 61.6, 57.3, 56.7, 55.9, 51.0, 46.0, 30.8, 29.6, 12.9.

Akuammiline (5): white solid, ^{1}H NMR ($CDCl_3$, 400 MHz) δ 7.66 (1H, d, *J* = 7.4 Hz), 7.59 (1H, d, *J* = 7.7 Hz), 7.31 (1H, td, *J* = 7.5, 1.1 Hz), 7.15 (1H, td, *J* = 11.3, 0.8 Hz), 5.50 (1H, q, *J* = 7.1 Hz), 4.62 (1H, d, *J* = 4.5 Hz), 4.11 (1H, d, *J* = 17.3 Hz), 3.77 (3H, s), 3.65-3.56 (2H, m), 3.52 (2H, m), 3.15 (1H, d, *J* = 17.3 Hz), 3.69-2.54 (2H, m), 2.49 (1H, ddd, *J* = 14.6, 4.9, 2.5 Hz), 2.13 (1H, dd *J* = 14.8, 3.4 Hz), 1.91 (1H, dd, *J* = 14.5, 2.4 Hz), 1.66 (3H, dd, *J* = 7.2, 2.3 Hz), 1.58 (3H, s); ^{13}C NMR ($CDCl_3$, 100 MHz) δ 189.4, 171.4, 169.3, 155.4, 144.8, 139.3, 128.1, 126.0, 125.4, 121.1, 120.2, 66.2, 59.2, 58.7, 54.4, 53.8, 52.2, 51.8, 37.7, 37.0, 30.9, 20.1, 13.4.

Picraline (6): off-white solid, ^{1}H NMR ($CDCl_3$, 400 MHz) δ 7.44 (1H, d, *J* = 7.5 Hz), 7.06 (1H, td, *J* = 7.6, 1.1 Hz), 6.84 (1H, t, *J* = 7.5 Hz), 6.74 (1H, d, *J* = 7.8 Hz), 5.4 (1H, q, *J* = 7.0 Hz), 4.87 (1H, s), 4.77 (1H, d, *J* = 2.4 Hz), 4.57 (1H, d, *J* = 11.0 Hz), 3.90 (1H, d, *J* = 11.0 Hz), 3.81 (1H, d, *J* = 17.8 Hz), 3.70 (3H, s), 3.63 (1H, m), 3.32 (1H, m), 3.23 (1H, d, *J* = 14.0 Hz), 3.14 (1H, d, 18.0 Hz), 2.47 (1H, dd, *J* = 14.0, 2.6 Hz), 2.01 (2H, m), 1.61 (3H, dd, *J* = 7.1, 1.9 Hz), 1.54 (3H, s); ^{13}C NMR ($CDCl_3$, 100 MHz) δ 172.2, 170.0, 148.2, 137.2, 133.7, 127.9, 127.6, 121.0, 120.9, 111.2, 107.0, 87.2, 67.1, 56.2, 52.9, 51.6, 51.5, 46.6, 44.3, 35.6, 22.0, 20.1, 13.2.

Primary and Secondary Receptor Screening. We had the ability to submit **1** and **3**-**6**, but unfortunately not **2**, to the Psychoactive Drug Screening Program (UNC-Chapel Hill) as dry powders to be evaluated using standard protocols. Primary screening was conducted at 10 μM (DMSO) against the “Comprehensive Screen” panel consisting of 37 different GPCR, ion channel, and transporter targets. Assays producing >50% inhibition

of radioligand binding were further investigated in secondary binding assays using a 12-point concentration-response curve to determine binding affinity (*K*i).

Cell Culture. HEK293 cells (RRID:CVCL_0045, Life Technologies, Grand Island, NY, USA) were maintained in DMEM supplemented 10% FBS. CHO-K1-human δ opioid receptor (δOR PathHunter β-arrestin 2 cells and CHO-K1-human μ opioid receptor (μOR) PathHunter β-arrestin 2 cells stably expressing the δOR or μOR and β-arrestin 2 (RRID:CVCL_KY70, RRID:CVCL_KY68, DiscoverX, Fremont, CA, USA) were maintained in F12 media supplemented with 10% FBS and containing 800 μg/mL geneticin and 300 μg/mL hygromycin. U2OS-human κ opioid receptor (κOR) PathHunter β-arrestin 2 cells stably expressing the κOR and β-arrestin 2 (RRID:CVCL_LA97, DiscoverX, Fremont, CA, USA) were maintained in McCoy's 5A media supplemented with 10% FBS and containing 500 μg/mL geneticin and 250 μg/mL hygromycin. All cell lines were maintained in T75 flasks under sterile conditions and kept at 37 °C and 5% CO_2. During passaging, cells were dislodged from the flask following a 3-minute incubation with 0.25% trypsin, and sub cultivated at ratios of 1:10 (HEK293), 1:5 (CHO) and 3:10 (U2OS).

Competitive Radioligand Binding Assay. Binding assays were performed on membranes isolated from CHO cells stably expressing the δOR or μOR and from U2OS cells stably expressing the κOR (DiscoverX) as previously described using tritiated radioligands ([^{3}H]DAMGO, [^{3}H]U69,593, [^{3}H]DPDPE for μOR, κOR, δOR, respectively).[39]

GloSensor cAMP Inhibition Assay. cAMP inhibition assays were performed as previously described in HEK293 cells transiently transfected with pGloSensor22F-cAMP (Promega, Madison, WI, USA) and either FLAG-mouse δOR, HA-mouse μOR, or FLAG-mouse κOR.[40]

PathHunter β-arrestin2 Recruitment Assay. β-arrestin recruitment assays were performed as previously described using CHO or U2OS cells (CHO-K1-human δOR, CHO-K1-human μOR, or U2OS-human κOR PathHunter β-arrestin 2 cells, DiscoverX).[40]

Animals. Wildtype C57Bl/6N mice (24 male, 24 female; 7-8-weeks old) were purchased from Envigo (Indianapolis, IN) and were acclimated to the facility and to handling for 1 week prior to any experimental procedures. See supplemental data for information on subject groups for drug testing (**Supplementary Table 8**). All mice were housed on a 12-hour light (21:30-9:30)/12-hour dark cycle under controlled temperature (21-23 °C) with ad libitum food access. All experiments were conducted between 10:30-15:00 in a well-lit room. At a

minimum, mice were given 2 days between experiments to recover from thermal stimuli. All experimental procedures were approved by the Purdue Animal Care and Use Committee of Purdue University under protocol #1605001408.

Tail Flick Thermal Nociception Assay. Antinociception was measured as previously described.[41] On the first day of the experiment, mice were habituated to handling restraint; a black washcloth was used to restrain the mice during the experimentation. On the following days of drug testing, a radiant heat tail-flick apparatus (Columbus Instruments, Columbus, OH, USA) was set to a beam intensity of 7-9 as this intensity yielded reproducible responses between 2-3 seconds. On each test day, a baseline tail flick response was first obtained for each mouse. The cutoff time for testing was calculated as 3 times this baseline response time. A saline injection was then administered (s.c. or p.o.) and after 30 minutes, tail flick responses were collected again. Drugs were then administered (s.c. or p.o.), and tail flick responses were collected at various time points following administration. All measurements were collected in duplicate by testing two different regions on the mouse's tail.

Hot Plate Thermal Nociception Assay. On the first day of the experiment, mice were habituated to the hotplate apparatus (Columbus Instruments, Columbus, OH, USA) for 1-2 minutes (while the hotplate was turned off). On the following days of testing, the hotplate was maintained at a temperature of 55 ± 0.5 °C. On each test day, a single baseline time for latency to demonstrate nociceptive behavior was first obtained for each mouse. Behavior considered a positive nociceptive response was fore or hind paw licking, jumping, or non-explorative rearing. Upon demonstrating this behavior, the mouse was immediately removed from the apparatus. The cutoff time for testing was calculated as 3 times the baseline response time. A saline injection was then administered (s.c. or p.o.) and after 30 minutes, hot plate latency responses were collected again. Drugs were then administered (s.c. or p.o.), and hot plate latency responses were collected following administration at various time points. All measurements were collected only once to avoid damage to paws.

Statistics. All data was analyzed using GraphPad 8 (GraphPad Prism software, La Jolla, CA) and is presented as means ± SEM. For *in vitro* findings, composite figures consisted of one curve averaged from three, independent assays. In these independent assays, PathHunter β-arrestin recruitment and radioligand binding assays were run in duplicate, and GloSensor cAMP assays were run in triplicate. Data from each independent signaling assay was normalized to a positive control before being averaged and added to the composite figure. For nociception assays, significance was calculated via one-way, repeated measures ANOVA with Sidak's

multiple comparison's test to compare saline treatment with drug treatment at multiple time points. For any nociception assays where only one time point was tested, a paired t-test was used to assess significance between saline and drug treatment. Nociception data is represented as percent maximal possible effect (%MPE) (calculated as % MPE= (treatment response time – baseline response time)/(cutoff time – baseline response time) * 100) and is normalized (drug treatment %MPE – saline treatment %MPE). Statistical measures and values for all nociception assays are summarized in **Supplementary Tables 9-11**.

ASSOCIATED CONTENT

Supporting Information

The Supporting Information is available free of charge at [[Insert Address Here]]

Tables comparing isolated and literature 13C NMR shifts; binding affinity data from PDSP; nociception subject groups; nociception statistics summary; ^{1}H and ^{13}C NMR spectra of all alkaloids.

AUTHOR INFORMATION

Corresponding Authors

Andrew P. Riley – Department of Pharmaceutical Sciences, College of Pharmacy, University of Illinois at Chicago, Chicago Illinois 60612, United States; Email: apriley@uic.edu

Richard M. van Rijn – *Department of Medicinal Chemistry and Molecular Pharmacology, College of Pharmacy, Purdue Institute for Drug Discovery, Purdue Institute for Integrative Neuroscience, Purdue Interdisciplinary Life Sciences Graduate Program, Purdue University, West Lafayette, Indiana 47907, United States*

Authors

Simone M. Creed – *Department of Pharmaceutical Sciences, College of Pharmacy, University of Illinois Chicago, Chicago, Illinois 60612, United States*

Anna M. Gutridge – *Department of Medicinal Chemistry and Molecular Pharmacology, College of Pharmacy, Purdue University, West Lafayette, Indiana 47907, United States*

Malaika D. Argade – *Department of Pharmaceutical Sciences, College of Pharmacy, University of Illinois Chicago, Chicago, Illinois 60612, United States*

Madeline R. Hennessy – *Department of Pharmaceutical Sciences, College of Pharmacy, University of Illinois Chicago, Chicago, Illinois 60612, United States*

J. Brent Friesen – *Department of Pharmaceutical Sciences and 2Program for Collaborative Research in the Pharmaceutical Sciences (PCRPS), College of Pharmacy, University of Illinois Chicago, Chicago, Illinois 60612, United States*

Guido F. Pauli – *Department of Pharmaceutical Sciences and 2Program for Collaborative Research in the Pharmaceutical Sciences (PCRPS), College of Pharmacy, University of Illinois Chicago, Chicago, Illinois 60612, United States*

Notes

The authors declare no competing financial interest.

ACKNOWLEDGEMENTS

This research was supported by funds awarded to APR by the National Center for Advancing Translational Sciences (KL2TR002002), to MRH by National Center for Complementary and Integrative Health (AT007533), to AMG by the American Foundation for Pharmaceutical Education Pre-doctoral Fellowship, and to RMvR by the National Institute on Alcohol Abuse and Alcoholism (AA025368, AA026949, and AA026675) and the National Institute on Drug Abuse (DA045897) of the National Institutes of Health. Receptor binding profiles were generously provided by the National Institute of Mental Health's Psychoactive Drug Screening Program, Contract # HHSN-271-2018-00023-C (NIMH PDSP). The NIMH PDSP is Directed by Bryan L. Roth at the University of North Carolina at Chapel Hill and Project Officer Jamie Driscoll at NIMH, Bethesda MD, USA. The content is solely the responsibility of the authors and does not necessarily represent the official views of the NIH. The TOC graphic was created with BioRender.com.

REFERENCES

1. Jones, M. R.; Viswanath, O.; Peck, J.; Kaye, A. D.; Gill, J. S.; Simopoulos, T. T., A Brief History of the Opioid Epidemic and Strategies for Pain Medicine. *Pain Ther.* **2018,** *7*, 13-21.
2. Hylands-White, N.; Duarte, R. V.; Raphael, J. H., An overview of treatment approaches for chronic pain management. *Rheumatol. Int.* **2017,** *37*, 29-42.
3. Volkow, N. D.; Blanco, C., The changing opioid crisis: development, challenges and opportunities. *Mol. Psychiatry* **2020**.
4. Goldberg, D. S.; McGee, S. J., Pain as a global public health priority. *BMC Public Health* **2011,** *11*, 770.
5. Ho, A.; Nair, S., Chapter Nine - Global Chronic Pain: Public and Population Health Responses. In *Developments in Neuroethics and Bioethics*, Buchman, D. Z.; Davis, K. D., Eds. Academic Press: 2018; Vol. 1, pp 171-189.
6. Marshall, B.; Bland, M. K.; Hulla, R.; Gatchel, R. J., Considerations in addressing the opioid epidemic and chronic pain within the USA. *Pain Manag.* **2019,** *9*, 131-138.
7. Nana Wilson; Mbabazi Kariisa; Puja Seth; Herschel Smith IV, M. N. L. D., Drug and Opioid-Involved Overdose Deaths–United States, 2017-2018. 2020; Vol. 69, pp 290-297.

8. Dowell, D.; Haegerich, T. M.; Chou, R., CDC Guideline for Prescribing Opioids for Chronic Pain-United States, 2016. *JAMA* **2016,** *315*, 1624-1645.
9. Bohnert, A. S. B.; Guy, G. P., Jr.; Losby, J. L., Opioid Prescribing in the United States Before and After the Centers for Disease Control and Prevention's 2016 Opioid Guideline. *Ann. Intern. Med.* **2018,** *169*, 367-375.
10. Gross, J.; Gordon, D. B., The Strengths and Weaknesses of Current US Policy to Address Pain. *Am. J. Public Health* **2019,** *109*, 66-72.
11. Boyer, E. W.; Babu, K. M.; Adkins, J. E.; McCurdy, C. R.; Halpern, J. H., Self-treatment of opioid withdrawal using kratom (Mitragynia speciosa korth). *Addiction* **2008,** *103* , 1048-1050.
12. Toce, M. S.; Chai, P. R.; Burns, M. M.; Boyer, E. W., Pharmacologic Treatment of Opioid Use Disorder: a Review of Pharmacotherapy, Adjuncts, and Toxicity. *J. Med. Toxicol.* **2018,** *14*, 306-322.
13. Newman, D. J.; Cragg, G. M., Natural Products as Sources of New Drugs over the Nearly Four Decades from 01/1981 to 09/2019. *J. Nat. Prod.* **2020,** *83*, 770-803.
14. Gouveia, D. N.; Guimaraes, A. G.; Santos, W.; Quintans-Junior, L. J., Natural products as a perspective for cancer pain management: A systematic review. *Phytomedicine* **2019,** *58*, 152766.
15. Turk, D. C.; Wilson, H. D.; Cahana, A., Treatment of chronic non-cancer pain. *Lancet* **2011,** *377*, 2226-35.
16. Erharuyi, O.; Falodun, A.; Langer, P., Medicinal uses, phytochemistry and pharmacology of *Picralima nitida* (Apocynaceae) in tropical diseases: a review. *Asian Pac. J. Trop. Med.* **2014,** *7*, 1-8.
17. Menzies, J. R.; Paterson, S. J.; Duwiejua, M.; Corbett, A. D., Opioid activity of alkaloids extracted from Picralima nitida (fam. Apocynaceae). *Eur J Pharmacol* **1998,** *350*, 101-108.
18. Dapaah, G.; Koffuor, G. A.; Mante, P. K.; Ben, I. O., Antitussive, expectorant and analgesic effects of the ethanol seed extract of Picralima nitida (Stapf) Th. & H. Durand. *Res. Pharm. Sci.* **2016,** *11*, 100-112.
19. Duwiejua, M.; Woode, E.; Obiri, D. D., Pseudo-akuammigine, an alkaloid from Picralima nitida seeds, has anti-inflammatory and analgesic actions in rats. *J. Ethnopharmacol.* **2002,** *81*, 73-79.
20. Ama-Asamoah, R.; Kapadia, G. J.; Lloyd, H. A.; Sokoloski, E. A., Picratidine, a New Indole Alkaloid from Picralima nitida Seeds. *J. Nat. Prod.* **1990,** *53*, 975-977.
21. Møller, B. L.; Seedorff, L.; Nartey, F., Alkaloids of Picralima nitida. *Phytochemistry* **1972,** *11*, 2620-2621.
22. Tane, P.; Tene, M.; Sterner, O., Picranitine, a new indole alkaloid from Picralima nitida (apocynaceae). *Bull. Chem. Soc. Ethiop.* **2002,** *16*, 165-168.
23. Okunji, C. O.; Iwu, M. M.; Ito, Y.; Okunji, C. O.; Iwu, M. M.; Smith, P. L., Preparative separation of indole alkaloids from the rind of Picralima nitida (Stapf) T. Durand & H. Durand by pH-zone-refining countercurrent chromatography. *J. Liq. Chromatogr. Relat. Technol.* **2005,** *28*, 775-783.
24. Ito, Y., Golden rules and pitfalls in selecting optimum conditions for high-speed counter-current chromatography. *J. Chromatogr. A* **2005,** *1065*, 145-168.
25. Ito, Y., pH-zone-refining counter-current chromatography: origin, mechanism, procedure and applications. *J. Chromatogr. A* **2013,** *1271*, 71-85.
26. Ito, Y.; Ma, Y., pH-zone-refining countercurrent chromatography. *J. Chromatogr. A* **1996,** *753*, 1-36.
27. Fang, L.; Zhou, J.; Lin, Y.; Wang, X.; Sun, Q.; Li, J. L.; Huang, L., Large-scale separation of alkaloids from Gelsemium elegans by pH-zone-refining counter-current chromatography with a new solvent system screening method. *J. Chromatogr. A* **2013,** *1307*, 80-85.
28. Kotland, A.; Chollet, S.; Diard, C.; Autret, J. M.; Meucci, J.; Renault, J. H.; Marchal, L., Industrial case study on alkaloids purification by pH-zone refining centrifugal partition chromatography. *J. Chromatogr. A* **2016,** *1474*, 59-70.
29. Maurya, A.; Gupta, S.; Srivastava, S. K., Large-scale separation of antipsychotic alkaloids from Rauwolfia tetraphylla L. by pH-zone-refining fast centrifugal partition chromatography. *J. Sep. Sci.* **2013,** *36*, 407-413.
30. Zhou, J.; Du, S. Y.; Dong, H. J.; Fang, L.; Feng, J. H., Preparative Separation of Monoterpenoid Indole Alkaloid Epimers from Ervatamia yunnanensis Tsiang by pH-Zone-Refining Counter-Current Chromatography Combined with Preparative High-Performance Liquid Chromatography. *Molecules* **2019,** *24*.
31. Benayad, S.; Ahamada, K.; Lewin, G.; Evanno, L.; Poupon, E., Preakuammicine: A Long-Awaited Missing Link in the Biosynthesis of Monoterpene Indole Alkaloids. *Eur. J. Org. Chem.* **2016,** 1494-1499.
32. Jokela, R.; Lounasmaa, M., H-1- and C-13-NMR spectral data of five sarpagine-type alkaloids. *Heterocycles* **1996,** *43*, 1015-1020
33. Yamauchi, T.; Abe, F.; Chen, R. F.; Nonaka, G.; Santisuk, T.; Padolina, W. G., Alstonia .3. Alkaloids from the Leaves of Alstonia-Scholaris in Taiwan, Thailand, Indonesia and the Philippines. *Phytochemistry* **1990,** *29*, 3547-3552.

34. Gutridge, A. M.; Robins, M. T.; Cassell, R. J.; Uprety, R.; Mores, K. L.; Ko, M. J.; Pasternak, G. W.; Majumdar, S.; van Rijn, R. M., G protein-biased kratom-alkaloids and synthetic carfentanil-amide opioids as potential treatments for alcohol use disorder. *Br. J. Pharmacol.* **2020,** *177*, 1497-1513.
35. Case, R. J.; Franzblau, S. G.; Wang, Y.; Cho, S. H.; Soejarto, D. D.; Pauli, G. F., Ethnopharmacological evaluation of the informant consensus model on anti-tuberculosis claims among the Manus. *J Ethnopharmacol.* **2006,** *106*, 82-89.
36. Qiu, F.; Cai, G.; Jaki, B. U.; Lankin, D. C.; Franzblau, S. G.; Pauli, G. F., Quantitative purity-activity relationships of natural products: the case of anti-tuberculosis active triterpenes from Oplopanax horridus. *J. Nat. Prod.* **2013,** *76*, 413-419.
37. Inui, T.; Wang, Y.; Nikolic, D.; Smith, D. C.; Franzblau, S. G.; Pauli, G. F., Sesquiterpenes from Oplopanax horridus. *J. Nat. Prod.* **2010,** *73*, 563-567.
38. Choules, M. P.; Klein, L. L.; Lankin, D. C.; McAlpine, J. B.; Cho, S. H.; Cheng, J.; Lee, H.; Suh, J. W.; Jaki, B. U.; Franzblau, S. G.; Pauli, G. F., Residual Complexity Does Impact Organic Chemistry and Drug Discovery: The Case of Rufomyazine and Rufomycin. *J. Org. Chem.* **2018,** *83*, 6664-6672.
39. Cassell, R. J.; Mores, K. L.; Zerfas, B. L.; Mahmoud, A. H.; Lill, M. A.; Trader, D. J.; van Rijn, R. M., Rubiscolins are naturally occurring G protein-biased delta opioid receptor peptides. *Eur. Neuropsychopharmacol.* **2019,** *29*, 450-456.
40. Chiang, T.; Sansuk, K.; van Rijn, R. M., beta-Arrestin 2 dependence of delta opioid receptor agonists is correlated with alcohol intake. *Br. J. Pharmacol.* **2016,** *173*, 332-43.
41. van Rijn, R. M.; Brissett, D. I.; Whistler, J. L., Emergence of functional spinal delta opioid receptors after chronic ethanol exposure. *Biol. Psychiatry* **2012,** *71*, 232-238.

FIGURES AND TABLES

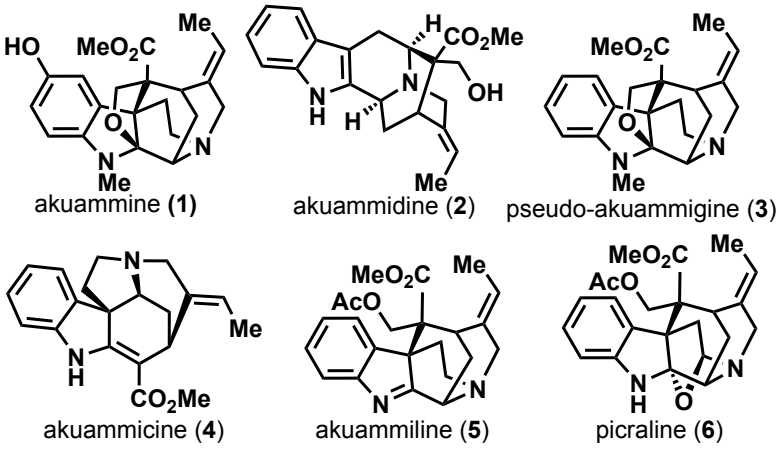

Figure 1. Structures of the akuamma alkaloids isolated from *P. nitidia*.

Solvent System		Pseudo-akuammigine (3)	Akuammicine (4)	Akuammiline (5)	Picraline (6)
1:1:1:1 Hex/EtOAc/ MeOH/H_2O	K_{acid}	<<0.01	<<0.01	<<0.01	<<0.01
	K_{base}	22.25	13.57	0.23	1.27
3:7:3:7 Hex/EtOAc/ MeOH/H_2O	K_{acid}	<<0.01	<<0.01	<<0.01	0.03
	K_{base}	32.27	>>100	2.53	4.22
1:1 EtOAc/H_2O	K_{acid}	0.10	0.02	0.03	0.15
	K_{base}	51.93	14.73	28.24	17.13
2:2:3 MTBE/ACN/ H_2O	K_{acid}	2.22	0.64	0.27	1.50
	K_{base}	86.99	21.62	5.61	10.65
3:1.5:4 MTBE/ACN/ H_2O	K_{acid}	0.25	0.13	0.05	0.38
	K_{base}	30.86	65.95	6.82	5.78

Table 1. Partition coefficients of akuamma alkaloids in CCC solvent systems. The K_{acid} and K_{base} for each akuamma alkaloid was calculated by taking $AUC_{upper\ phase}/AUC_{lower\ phase}$ as observed by HPLC for respective pH conditions.

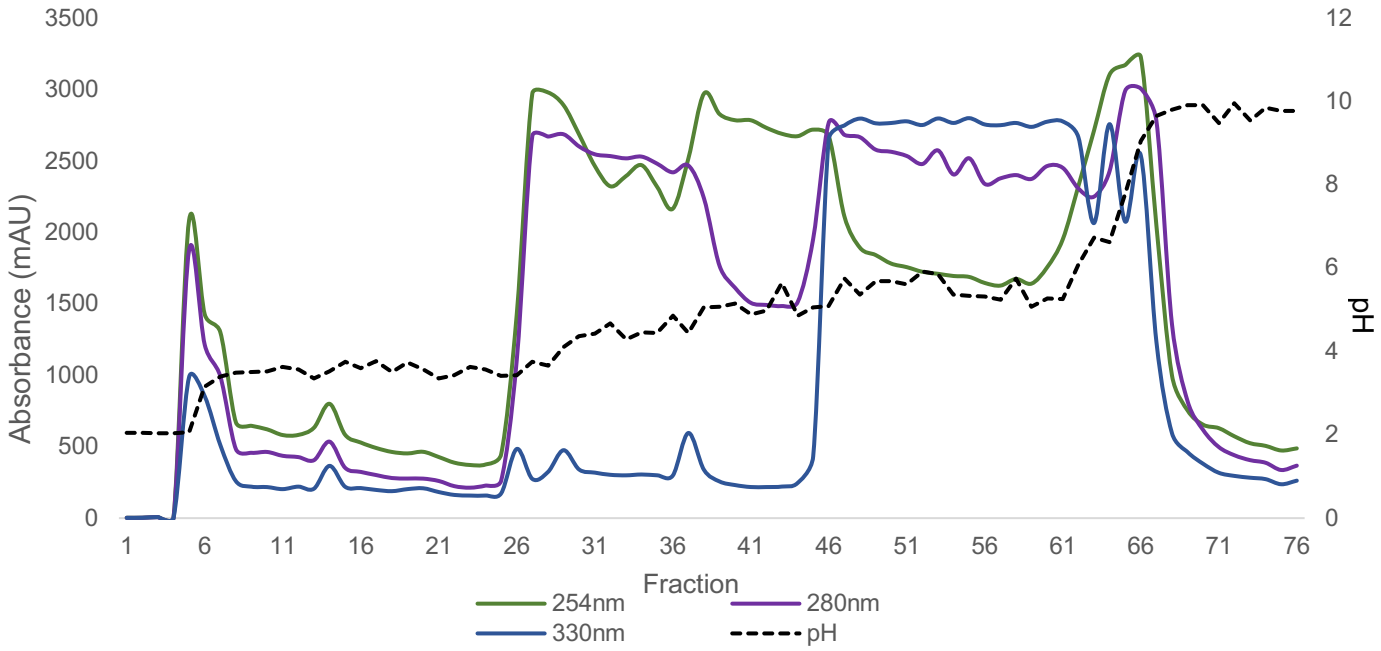

Figure 2. pH-zone-refining countercurrent chromatography chromatogram of akuamma alkaloid DCM extract. Elution of the alkaloids akuammiline (**5**) and picraline (**6**) occurred between high pH 3 to low-mid pH 4 range. Elution of pseudo-akuammigine (**3**) occurred between mid pH 4 to low pH 5. Elution of akuammicine (**4**) occurred between low to high pH 5.

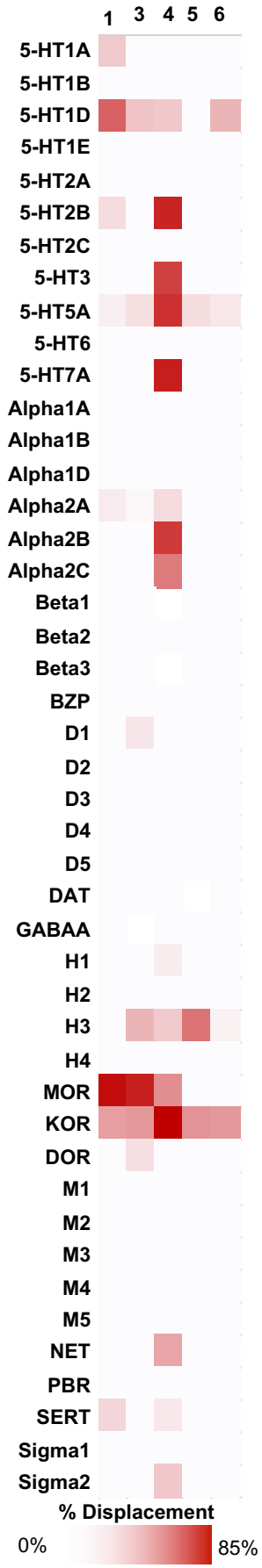

Figure 3. Receptor binding profiles of akuamma alkaloids. The akuamma alkaloids akuammine (**1**), pseudo-akuammigine (**3**), akuammicine (**4**), akuammiline (**5**), and picraline (**6**) were assessed at 10 μM for their ability to displace radiolabeled ligands from membranes expressing individual receptors. The heatmap represents mean displacement of radioligand from four replicates.

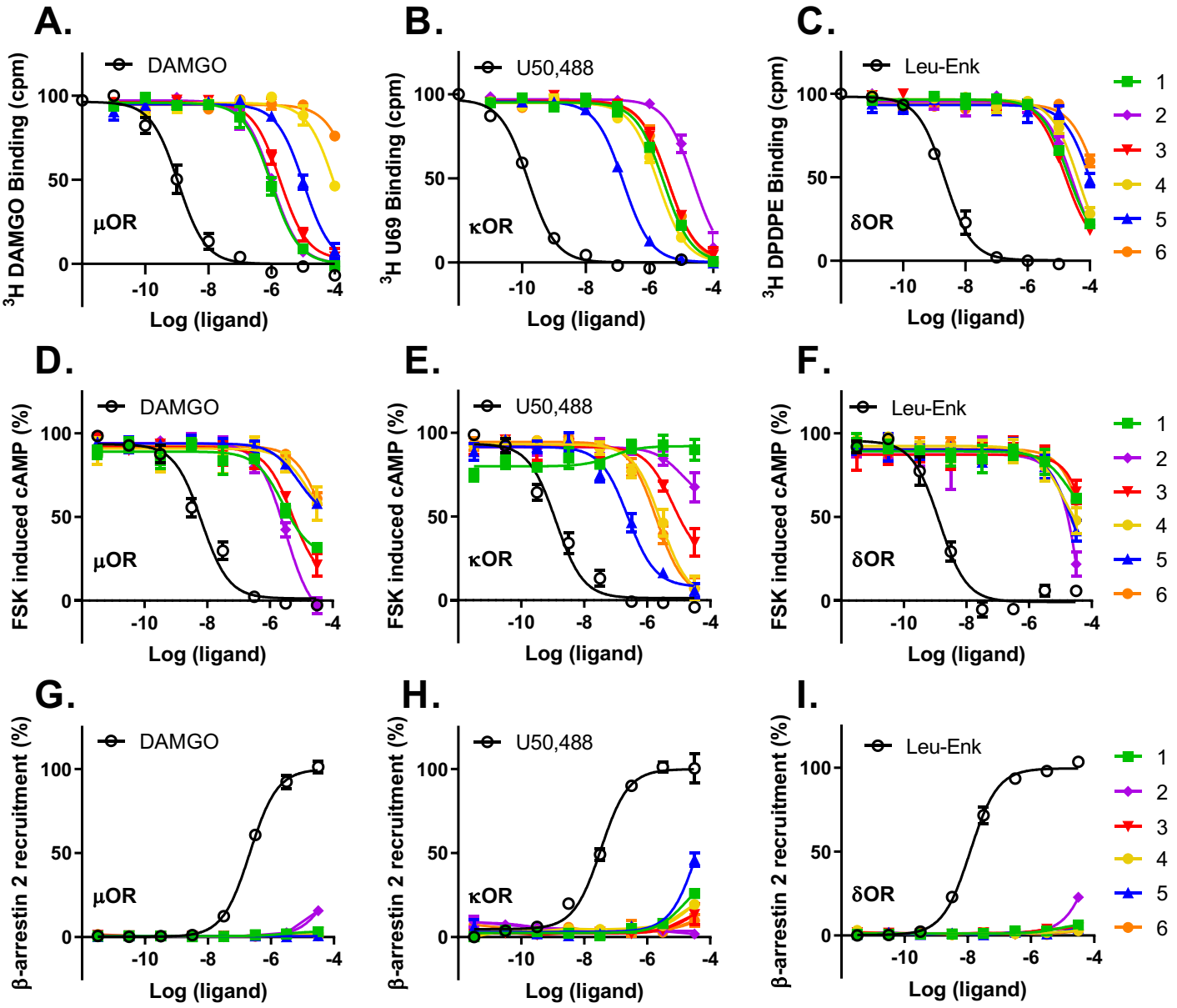

Figure 4. Pharmacological characterization of akuamma alkaloids at μOR, κOR, and δORs. The akuamma alkaloids akuammine (**1**), akuammidine (**2**), pseudo-akuammigine (**3**), akuammicine (**4**), akuammiline (**5**), and picraline (**6**) were characterized for binding affinity using [^{3}H]DAMGO, [^{3}H]U69,593 and [^{3}H]DPDPE (**A, B, C**), inhibition of forskolin-induced cAMP in a Glo-sensor assay in transfected HEK-293 cells (**D, E, F)** and the ability of the alkaloids to recruit β-arrestin 2 in a PathHunter assay. (**G, H, I**) at μOR (**A, D, G**), κOR (**B, E, H**), and δOR (**C, F, I**). All curves are representative of the averaged values from a minimum of 3 independent assays.

Compounds	Binding		cAMP			β-arrestin 2	
μOR	**pK_i**	**K_i (μM)**	**pIC_{50}**	**IC_{50} (μM)**	**α**	**pEC_{50}**	**α**
DAMGO	-9.5 ± 0.1 (1)	0.00035	-8.2 ± 0.1 (4)	0.0066	100	-6.7 ± 0.1 (3)	100
1	-6.5 ± 0.1 (3)	0.30	-5.6 ± 0.2 (4)	2.60	62 ± 6	ND (3)	ND
2	-6.5 ± 0.1 (3)	0.32	-5.5 ± 0.1 (3)	3.14	94 ± 6	ND (3)	ND
3	-6.2 ± 0.1 (3)	0.59	-5.3 ± 0.1 (4)	5.24	82 ± 7	ND (3)	ND
4	-5.5 ± 0.1 (3)	3.31	-5.1 ± 0.2 (3)	8.24	45 ± 7	ND (3)	ND
5	-4.5 ± 0.1 (3)	30.7	-4.7 ± 0.8 (3)	18.7	50 ± 40	ND (3)	ND
6	ND (3)	132	ND (3)	45.0	ND	ND (3)	ND
κOR	**pK_i**	**K_i (μM)**	**pIC_{50}**	**IC_{50} (μM)**	**α**	**pEC_{50}**	**α**
U50,488	-10.0 ± 0.1(1)	0.000094	-8.9 ± 0.1 (6)	0.0015	100	-7.5 ± 0.1 (3)	100
1	-5.8 ± 0.1 (3)	1.68	ND (4)	0.073	ND	ND (3)	35 ± 6
2	-4.8 ± 0.1 (3)	14.2	ND (5)	ND	ND	ND (3)	ND
3	-5.6 ± 0.1 (3)	2.25	-5.2 ± 0.2 (6)	6.46	69 ± 8	ND (3)	20 ± 20
4	-7.1 ± 0.1 (3)	0.089	-6.6 ± 0.1 (4)	0.24	84 ± 4	-4.4 ± 0.4 (3)	50 ± 10
5	-6.0 ± 0.1 (3)	1.11	-5.6 ± 0.1 (4)	2.71	92 ± 6	ND (3)	30 ± 12
6	-5.6 ± 0.1 (3)	2.38	-5.7 ± 0.1 (4)	1.97	92 ± 5	ND (3)	ND
δOR	**pK_i**	**K_i (μM)**	**pIC_{50}**	**IC_{50} (μM)**	**α**	**pEC_{50}**	**α**
Leu-Enk	-8.9 ± 0.1 (1)	0.0012	-8.9 ± 0.1 (4)	0.0014	100	-7.9 ± 0.1 (3)	100
1	-5.0 ± 0.1 (3)	10.4	-4.7 ± 0.8 (3)	20.3	50 ± 35	ND (3)	ND
2	-4.8 ± 0.1 (3)	15.0	-4.8 ± 0.4 (3)	15.4	90 ± 30	ND (3)	ND
3	-5.1 ± 0.1 (3)	8.37	ND (3)	95.6	ND	ND (3)	ND
4	-4.6 ± 0.1 (3)	23.2	-4.9 ± 0.4 (3)	12.4	60 ± 20	ND (3)	ND
5	-4.2 ± 0.6 (3)	60.3	-4.6 ± 0.5 (3)	24.4	90 ± 50	ND (3)	ND
6	-4.0 ± 0.9 (3)	98.8	ND (3)	ND	ND	ND (3)	ND

Table 2. Summary of akuamma alkaloids *in vitro* characterization at opioid receptors.

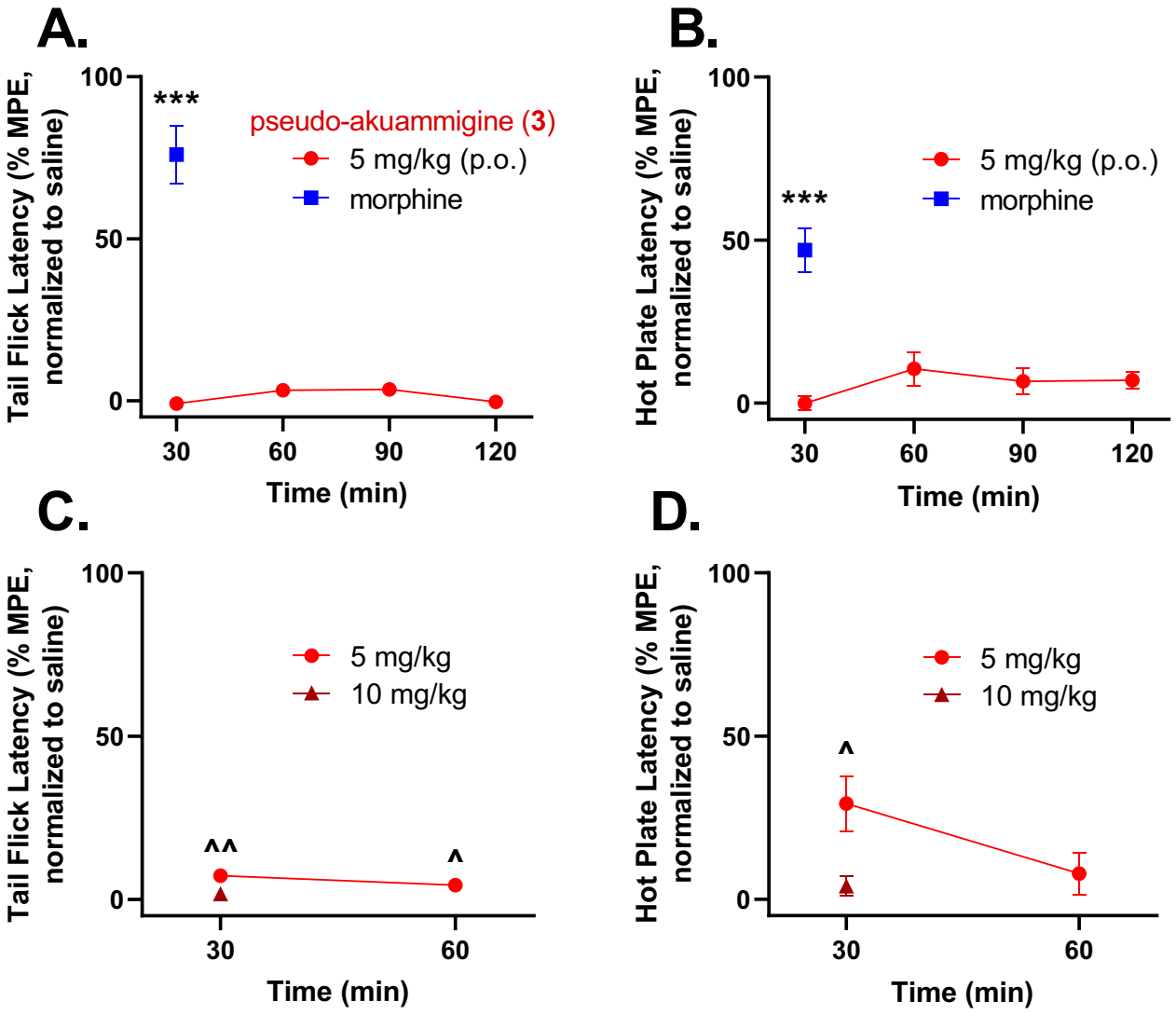

Figure 5. Effects of pseudo-akuammigine in mouse models of thermal nociception. Antinociception by pseudo-akuammigine (**3**) was tested at doses of 5 mg/kg (p.o., n=16) (**A-B**) and 5 and 10 mg/kg (s.c., n=8) (**C-D**) in C57BL/6 mice via the tail flick assay (**A** and **C**) and the hot plate assay (**B** and **D**) at various time points. Morphine (6 mg/kg, s.c., n=8) served as a positive control (**A-B**). All data is expressed as maximum possible effect (%MPE) normalized to a saline baseline (treatment – saline baseline). For the 5 mg/kg doses, ^P < 0.05 vs. vehicle and ^^P < 0.01 vs vehicle. For morphine, ***P < 0.001 vs. vehicle. Morphine and 10 mg/kg alkaloid **3** data was analyzed with a paired t-test. Data for 5 mg/kg alkaloid **3** (p.o. and s.c.) was analyzed with one-way, repeated measures ANOVA followed by Sidak's multiple comparisons post-test.

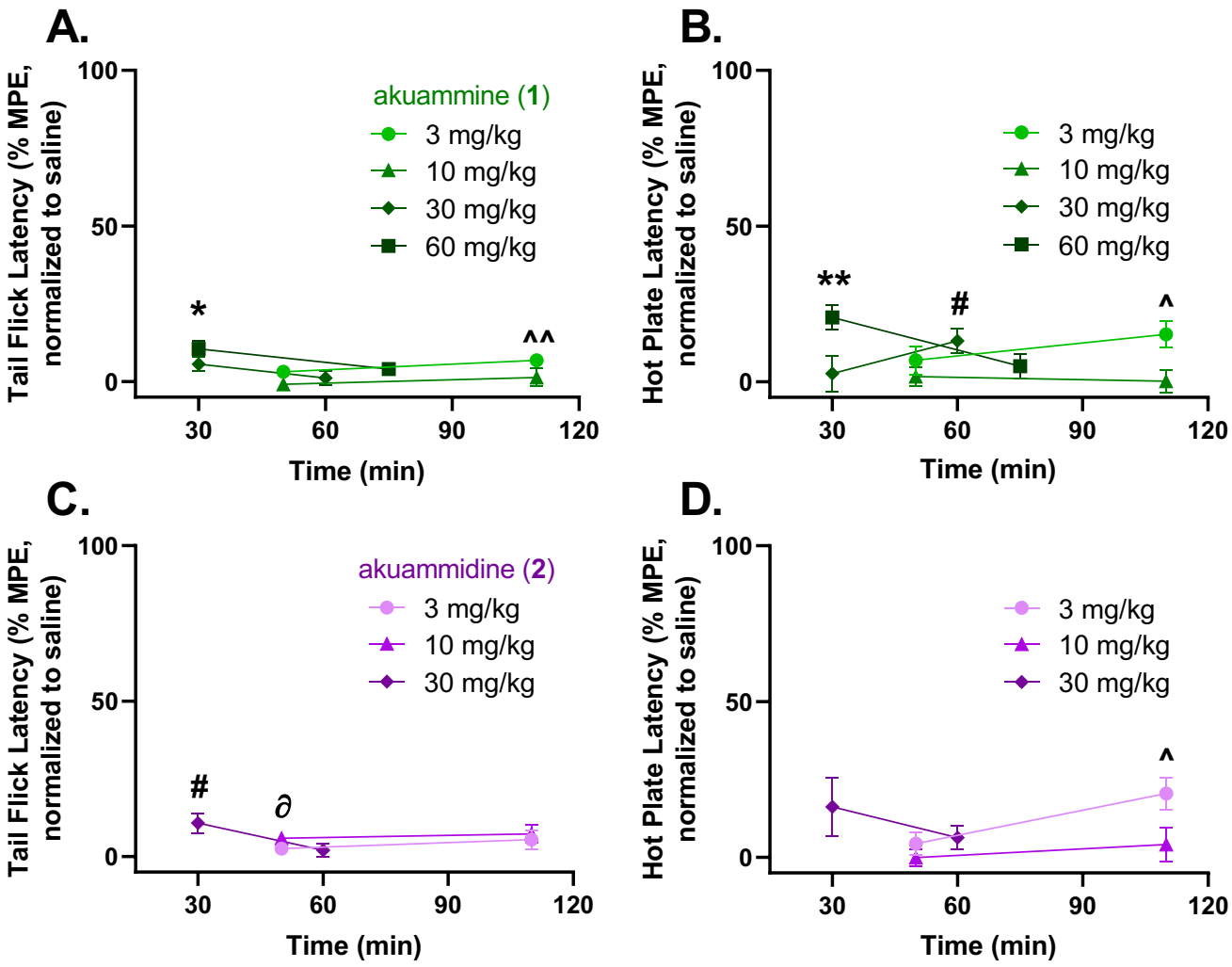

Figure 6. Effects of akuammine and akuammidine in mouse models of thermal nociception. Antinociception by akuammine (**1**) (3, 10, 30, and 60 mg/kg (s.c.)), **A-B**) and akuammidine (**2**) (3, 10, and 30 mg/kg (s.c.)), **C-D**) was assessed in C57BL/6 mice (n=8, per alkaloid) via the tail flick assay (**A** and **C**) and the hot plate assay (**B** and **D**) at various time points. All data is expressed as maximum possible effect (%MPE) normalized to a saline baseline (treatment – saline baseline). For the 3 mg/kg doses, ^P < 0.05 vs vehicle and ^^P < 0.01 vs vehicle. For the 10 mg/kg doses, statistical significance is indicated as $^{\partial}$P < 0.05 vs vehicle. For the 30 mg/kg doses, $^{\#}$P < 0.05 vs vehicle. For the 60 mg/kg doses, *P < 0.05 vs vehicle and **P < 0.01 vs vehicle. Data was analyzed with one-way, repeated measures ANOVA followed by Sidak's multiple comparisons post-test.

TOC GRAPHIC

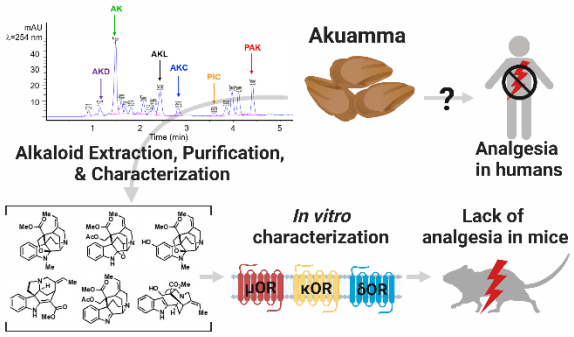
AK
AKD
AKL
AKC
PIC
PAK
mAU
λ=254 nm
Time (min)
Akuamma
?
Analgesia
in humans
Alkaloid Extraction, Purification,
& Characterization
In vitro
characterization
Lack of
analgesia in mice
μOR
κOR
δOR